J|A|C|S ARTICLES

Published on Web 02/25/2010

Intermolecular Protein−RNA Interactions Revealed by 2D $^{31}P-^{15}N$ Magic Angle Spinning Solid-State NMR Spectroscopy

Stefan Jehle,[†,||] Melanie Falb,[†] John P. Kirkpatrick,[†,⊥] Hartmut Oschkinat,[‡] Barth-Jan van Rossum,[‡] Gerhard Althoff,[§] and Teresa Carlomagno*[,†]

Computational and Structural Biology Unit, European Molecular Biology Laboratory, Meyerhofstrasse 1, 69117 Heidelberg, Germany, Leibniz-Institut für Molekulare Pharmakologie, Robert-Rössle-Strasse 10, 13125 Berlin, Germany, and Bruker Biospin, Im Silberstreifen 4, 76287 Rheinstetten, Germany

Received November 16, 2009; E-mail: teresa.carlomagno@embl.de

Abstract: The structural investigation of large RNP complexes by X-ray crystallography can be a difficult task due to the flexibility of the RNA and of the protein−RNA interfaces, which may hinder crystallization. In these cases, NMR spectroscopy is an attractive alternative to crystallography, although the large size of typical RNP complexes may limit the applicability of solution NMR. Solid-state NMR spectroscopy, however, is not subject to any intrinsic limitations with respect to the size of the object under investigation, with restrictions imposed solely by the sensitivity of the instrumentation. In addition, it does not require large, well-ordered crystals and can therefore be applied to flexible, partially disordered complexes. Here we show for the first time that solid-state NMR spectroscopy can be used to probe intermolecular interactions at the protein−RNA interface in RNP complexes. Distances between the ^{15}N nuclei of the protein backbone and the ^{31}P nuclei of the RNA backbone can be measured in TEDOR experiments and used as restraints in structure calculations. The distance measurement is accurate, as proven for the test case of the L7Ae−box C/D RNA complex, for which a crystal structure is available. The results presented here reveal the as yet unexplored potential of solid-state NMR spectroscopy in the investigation of large RNP complexes.

Introduction

Ribonucleoprotein (RNP) complexes are key players in cellular processes, where they play both regulatory and functional roles. Elucidation of the mechanisms of action of RNP complexes requires knowledge of their atomic structure, but RNP complexes often fail to crystallize due to their high degree of structural plasticity. Nuclear magnetic resonance spectroscopy (NMR) could assume a leading role in the structural investigation of RNP complexes, as it can cope with a high level of structural flexibility while being able to provide measurements of interatomic distances. However, NMR in solution is limited with respect to the size of the complexes under investigation, which should typically not exceed 100 kDa. In the past decade, solid-state NMR (ssNMR) spectroscopy has overcome the severe limitations in resolution and sensitivity that had dramatically limited its application to biomolecules in the past, and has been established as an important tool for studying large and poorly soluble biomolecules such as membrane proteins and protein fibrils.[1−4] The applicability of ssNMR to biological macromolecules is not limited to 100 kDa, as the line widths of ssNMR resonances do not depend on the size of the object under investigation. In addition, ssNMR does not require single crystals of particular size and hence is also applicable to RNP complexes that cannot be crystallized due to intrinsic flexibility. In spite of these advantages, the technique has not yet been applied to RNP complexes, probably due to the lack of appropriate experiments to study the RNA component of the complexes and the RNA−protein interactions.

In this work, we show for the first time that ssNMR spectroscopy can be successfully applied to measure interatomic RNA−protein distances in RNP complexes. In particular, we measure backbone−backbone distances between the phosphorus nuclei of the RNA and the nitrogen nuclei of the protein by exploiting the distance dependence of $^{31}P-^{15}N$ dipolar couplings in a TEDOR (transferred echo double resonance) experiment.[5,6] Such structural information is difficult to obtain by solution NMR spectroscopy even for small RNP complexes. In solution NMR, internuclear distances are typically measured between protons (NOE effects), but in the case of RNA−protein interfaces, the paucity of protons in the RNA backbone poses severe limitations on the distance information obtainable in

[†] European Molecular Biology Laboratory.
[‡] Leibniz-Institut für Molekulare Pharmakologie.
[§] Bruker Biospin.
[||] Current address: Leibniz-Institut für Molekulare Pharmakologie, Robert-Rössle-Strasse 10, 13125 Berlin, Germany.
[⊥] Current address: Department of Structural and Molecular Biology, University College London, Gower Street, London WC1E 6BT.

(1) Castellani, F.; van Rossum, B.; Diehl, A.; Schubert, M.; Rehbein, K.; Oschkinat, H. *Nature* **2002**, *420*, 98–102.
(2) Jaroniec, C. P.; MacPhee, C. E.; Bajaj, V. S.; McMahon, M. T.; Dobson, C. M.; Griffin, R. G. *Proc. Natl. Acad. Sci. U.S.A.* **2004**, *101*, 711–716.
(3) Jehle, S.; van Rossum, B.; Stout, J. R.; Noguchi, S. M.; Falber, K.; Rehbein, K.; Oschkinat, H.; Klevit, R. E.; Rajagopal, P. *J. Mol. Biol.* **2009**, *385*, 1481–1497.
(4) Wasmer, C.; Lange, A.; Van Melckebeke, H.; Siemer, A. B.; Riek, R.; Meier, B. H. *Science* **2008**, *319*, 1523–1526.
(5) Jaroniec, C. P.; Filip, C.; Griffin, R. G. *J. Am. Chem. Soc.* **2002**, *124*, 10728–10742.
(6) Hong, M.; Griffin, R. G. *J. Am. Chem. Soc.* **1998**, *120*, 7113–7114.

10.1021/ja909723f

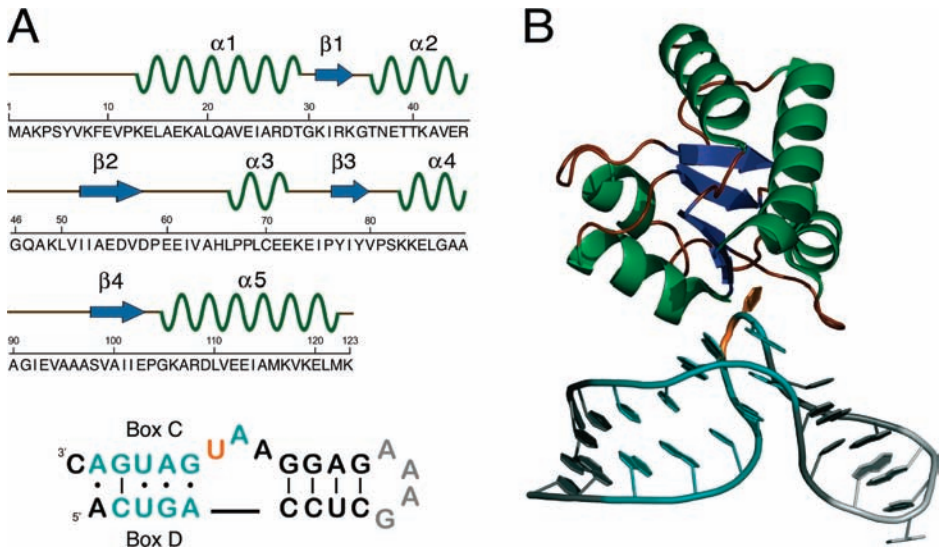

Figure 1. Sequence and structure of the L7Ae−box C/D RNA complex. (A) The amino acid sequence with secondary structure elements of L7Ae of *PF* (helix, green; β-sheets, blue; loop, red) and the nucleotide sequence of the box C/D RNA (box C/D, turquoise; stem, black; bulged-out U, orange) used in this study. (B) The X-ray structure of L7Ae in complex with the box C/D RNA of *AF* showing the K-turn motif of the RNA. The color code of the secondary structure elements of both protein and RNA is as in (A).

NOESY spectra. In ssNMR spectroscopy, however, heteronuclei can be directly correlated by dipolar-coupling-mediated correlation spectroscopy in differentially labeled samples.

As a test case, we use the complex between the box C/D RNA and the L7Ae protein of *Pyrococcus furiosus* (*PF*) (Figure 1A).[7] This complex is part of the large nucleolar 2′-O-methylation enzyme that processes rRNA by specific methylation at the 2′-OH position.[8] In archaea, the RNP particle is comprised of a small RNA (sRNA) and three proteins: L7Ae, Nop5p and fibrillarin, the last of which functions as the methyl transferase. The specific methylation guide sRNA contains two conserved sequences, box C and box D, and usually additional copies of these elements, boxes C′ and D′.[9−11] The particle is assembled hierarchically around boxes C and D, which first bind the L7Ae protein and second the Nop5p−fibrillarin complex.[12,13] Upon binding to the L7Ae protein, the box C/D RNA folds into a characteristic structural motif, called the kink-turn (K-turn). A crystal structure is available for the L7Ae of *Archaeoglobus fulgidis* (*AF*) in complex with a box C/D RNA (Figure 1B),[7] which makes the L7Ae−box C/D RNA complex an excellent model system for development of the ssNMR approach.

Materials and Methods

The L7Ae of *PF* was expressed and purified as described elsewhere[14] using M9 minimal medium with $^{15}NH_4Cl$ as the sole nitrogen source. The RNA was transcribed from a template by the T7 polymerase reaction and purified by preparative polyacrylamide gel electrophoresis. The resonance assignments for free and RNA-bound L7Ae were obtained from standard triple-resonance solution NMR experiments. The 2D solution-state $^{15}N-^{1}H$ correlation spectrum of Figure 2 was recorded at a field of 11.7 T and a temperature of 298 K, with acquisition times of 127 and 100 ms in t_2 and t_1, respectively. The resonance assignments for the ^{31}P, ^{13}C and ^{1}H nuclei of the U nucleotides of the RNA were obtained from a ^{13}C-edited NOESY spectrum and an HCP[15,16] spectrum acquired on a selectively labeled $^{13}C,^{15}N-U$ RNA construct in complex with L7Ae.

The solid-state NMR measurements were performed with a 400 MHz triple resonance (H/X/Y) wide-bore probe (Bruker, Karlsruhe, Germany). The probe is set to the desired frequency combination by means of exchangeable inserts. The insert fixes the frequency of the X channel, while the Y channel remains tunable over a broader range. The insert used for our experiments set the probe to $X/Y = {}^{31}P/{}^{15}N-{}^{65}Cu$. The sample for solid-state NMR contained ~16 mg L7Ae−box C/D RNA complex in a ZrO_2 rotor. The sample was prepared from a mixture of ^{15}N-labeled L7Ae and unlabeled RNA in a 1:1.5 molar ratio. The complex was precipitated in a SpeedVac by vapor diffusion from 40 mM HEPES buffer containing 14−16% PEG400 and 50 mM magnesium acetate as precipitants.[7,17]

The ssNMR line width at half-height for ^{15}N is ~50 Hz and is sufficiently narrow for structural studies (measured on the isolated side-chain ^{15}N resonance of H66 in L7Ae from a standard 1D CPMAS spectrum recorded with an acquisition time of 25 ms, ~83 kHz ^{1}H decoupling and magic angle spinning at 8 kHz). The ^{31}P line width in the ssNMR TEDOR correlation is 70 Hz. The π and $\pi/2$ pulse lengths for ^{15}N were 13 and 6.5 μs and for ^{31}P 8 and 4 μs, respectively. The TEDOR spectrum was recorded at a temperature of 280 K, with a MAS frequency of 8 kHz and ~85 kHz ^{1}H decoupling during indirect evolution and mixing. The acquisition times were 6 and 15 ms in t_1 and t_2, respectively (1536 scans). TEDOR mixing times of 3−14 ms were applied. The spectrum was processed with 2-fold linear prediction and squared sine-bell apodization in F_1. During cross-polarization from ^{1}H to ^{31}P at the $n = 1$ Hartmann−Hahn matching condition a 100−75% ramp on

(7) Moore, T.; Zhang, Y.; Fenley, M. O.; Li, H. *Structure* **2004**, *12*, 807–818.
(8) Reichow, S. L.; Hamma, T.; Ferre-D'Amare, A. R.; Varani, G. *Nucleic Acids Res.* **2007**, *35*, 1452–1464.
(9) Decatur, W. A.; Fournier, M. J. *J. Biol. Chem.* **2003**, *278*, 695–698.
(10) Kiss-Laszlo, Z.; Henry, Y.; Kiss, T. *EMBO J.* **1998**, *17*, 797–807.
(11) Tycowski, K. T.; Smith, C. M.; Shu, M. D.; Steitz, J. A. *Proc. Natl. Acad. Sci. U.S.A.* **1996**, *93*, 14480–14485.
(12) Szewczak, L. B. W.; Gabrielsen, J. S.; DeGregorio, S. J.; Strobel, S. A.; Steitz, J. A. *RNA* **2005**, *11*, 1407–1419.
(13) Watkins, N. J.; Dickmanns, A.; Luhrmann, R. *Mol. Cell. Biol.* **2002**, *22*, 8342–8352.
(14) Li, L.; Ye, K. Q. *Nature* **2006**, *443*, 302–307.
(15) Marino, J. P.; Schwalbe, H.; Anklin, C.; Bermel, W.; Crothers, D. M.; Griesinger, C. *J. Am. Chem. Soc.* **1994**, *116*, 6472–6473.
(16) Heus, H. A.; Wijmenga, S. S.; Vandeven, F. J. M.; Hilbers, C. W. *J. Am. Chem. Soc.* **1994**, *116*, 4983–4984.
(17) Martin, R. W.; Zilm, K. W. *J. Magn. Reson.* **2003**, *165*, 162–174.

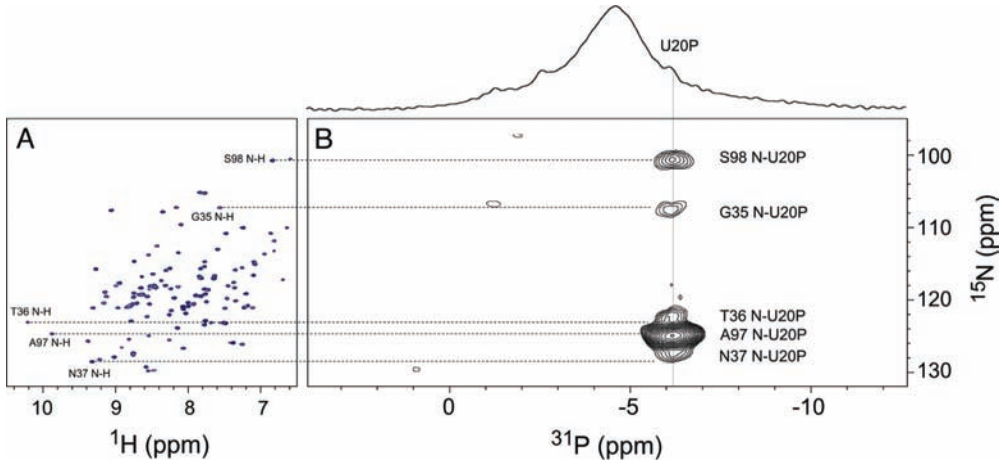

Figure 2. NMR analysis of the L7Ae−box C/D RNA complex (A) $^{15}N-^{1}H$ HSQC spectra of L7Ae bound to the box C/D RNA. The cross-peaks of residues in the RNA binding site are indicated and connected by dashed lines to the 2D $^{31}P-^{15}N$ TEDOR spectrum of L7Ae (^{15}N-labeled) in complex with the box C/D RNA (^{31}P), shown in (B). The ssNMR ^{31}P 1D spectrum of the L7Ae−box C/D RNA complex is shown on the top of the TEDOR 2D plot.

the ^{1}H channel was used. The applied fields were 60 kHz and 55 kHz on the ^{1}H and ^{31}P channels, respectively.

The TEDOR build-up curves were simulated using the SIMPSON software package (version 1.1.2). Calculations were performed for a rigid, isolated $^{31}P-^{15}N$ spin-pair, imposing a MAS frequency of 8.0 kHz and subjected to powder averaging (crystal file zcw376, 100 γ-angles). The different distances between the ^{31}P and ^{15}N spins were represented by a series of corresponding dipolar coupling strengths in the calculations. The TEDOR pulse sequence was simplified to its heteronuclear transfer part, using a starting operator I_x (^{31}P) and detection operator S^+ (^{15}N) to account for the amount of transfer. The simulation of each build-up curve took a few seconds of CPU time on a standard desktop PC (single core Pentium 4 CPU).

The starting model for generating the structure of *PF* L7Ae in complex with the box C/D RNA was derived by substituting the L7Ae protein in the *AF* L7Ae−box C/D RNA complex with that from the *PF* L7Ae−H/ACA RNA crystal structure.[14] In both complexes, the protein binds to the K-turn motif in the cognate RNA. The structures of the L7Ae proteins are very similar, with a backbone rmsd of 0.7 Å. The resulting model was then minimized using the following distance restraints: U20-$^{31}P-$G35-$^{15}N = 6.1 \pm 0.1$ Å; U20-$^{31}P-$T36-$^{15}N = 4.6 \pm 1.6$ Å; U20-$^{31}P-$N37-$^{15}N = 5.5 \pm 0.3$ Å; A19-$^{31}P-$A95-$^{15}N = >6.2$ Å; U20-$^{31}P-$A96-$^{15}N = >6.2$ Å; U20-$^{31}P-$A97-$^{15}N = 4.0 \pm 0.1$ Å; U20-$^{31}P-$S98-$^{15}N = 5.75 \pm 0.25$ Å. The restraints for G35, N37, A97, and S98, where the distances are well-defined from the TEDOR spectra, were incorporated as harmonic-well potentials, with force constants proportional to the uncertainty. The restraints for T36 (ill-defined due to spectral overlap) and A95 and A96 (minimum distance bounds) were included as steep-sided soft-square-well potentials. The minimization was performed using the Powell minimization engine in the structure calculation package Xplor-NIH[18] with the CHARMM22 force-field[19] and in an explicit shell of water molecules.

Results and Discussion

^{31}P (RNA)$-^{15}N$ (protein) distances were measured using a TEDOR[5,6] experiment for the complex of the box C/D RNA with the L7Ae protein of *PF* (Figure 1A). In this experiment, ^{31}P and ^{15}N nuclei separated by less than 5.0−5.5 Å (for a mixing time of 6−14 ms) are correlated via the dipolar-coupling mechanism (Figure S1). As shown in Figure 2, the TEDOR spectrum recorded with a mixing time of 12 ms indicates that only one phosphorus nucleus from the RNA backbone is in contact with the protein backbone and shows correlations to five backbone nitrogen nuclei. This is in perfect agreement with the crystal structure of the *AF* L7Ae−box C/D RNA complex,[7] which predicts four cross-peaks in the $^{31}P-^{15}N$ correlation spectrum between the phosphorus of U20 and the amide nitrogens of G35, T36, A97 and S98 ($^{31}P-^{15}N$ distance <5.5 Å) and demonstrates that the selective measurement of intermolecular $^{31}P-^{15}N$ distances in RNP complexes is indeed possible by ssNMR.

The next step in the analysis of the $^{31}P-^{15}N$ TEDOR correlation spectrum is the assignment of both the ^{15}N and ^{31}P resonances. The identification of the protein ^{15}N chemical shifts (CS) is a relatively simple task, as well-established methodologies are available for the assignment of protein backbone resonances by ssNMR.[20,21] In the test case used in this study, we relied on the assignment of the ^{15}N chemical shifts in solution. The equivalence of the solution-state and solid-state NMR CSs has previously been observed for other proteins[1,22−26] and is expected for all amino acids that are not involved in crystal packing contacts in the microcrystals of the ssNMR sample. As shown in Figure 2, there is an excellent correspondence between the solution CSs of the RNA-bound L7Ae and the peaks in the TEDOR spectrum, indicating that the nitrogens in close proximity to the RNA phosphorus belong to G35, T36, N37, A97, and S98. Indeed, amino-acids present at protein−RNA interfaces are usually not involved in crystal packing contacts, allowing for transfer of the easily assigned solution-state CSs to the solid-state NMR spectra. However,

(18) Schwieters, C. D.; Kuszewski, J. J.; Tjandra, N.; Clore, G. M. *J. Magn. Reson.* **2003**, *160*, 65–73.
(19) MacKerell, A. D.; et al. *J. Phys. Chem. B* **1998**, *102*, 3586–3616.
(20) Pauli, J.; Baldus, M.; van Rossum, B.; de Groot, H.; Oschkinat, H. *ChemBioChem* **2001**, *2*, 272–281.
(21) Hong, M. *J. Biomol. NMR* **1999**, *15*, 1–14.
(22) Igumenova, T. I.; Wand, A. J.; McDermott, A. E. *J. Am. Chem. Soc.* **2004**, *126*, 5323–5331.
(23) McDermott, A.; Polenova, T.; Bockmann, A.; Zilm, K. W.; Paulsen, E. K.; Martin, R. W.; Montelione, G. T. *J. Biomol. NMR* **2000**, *16*, 209–219.
(24) Franks, W. T.; Zhou, D. H.; Wylie, B. J.; Money, B. G.; Graesser, D. T.; Frericks, H. L.; Sahota, G.; Rienstra, C. M. *J. Am. Chem. Soc.* **2005**, *127*, 12291–12305.
(25) Marulanda, D.; Tasayco, M. L.; McDermott, A.; Cataldi, M.; Arriaran, V.; Polenova, T. *J. Am. Chem. Soc.* **2004**, *126*, 16608–16620.
(26) Marulanda, D.; Tasayco, M. L.; Cataldi, M.; Arriaran, V.; Polenova, T. *J. Phys. Chem. B* **2005**, *109*, 18135–18145.

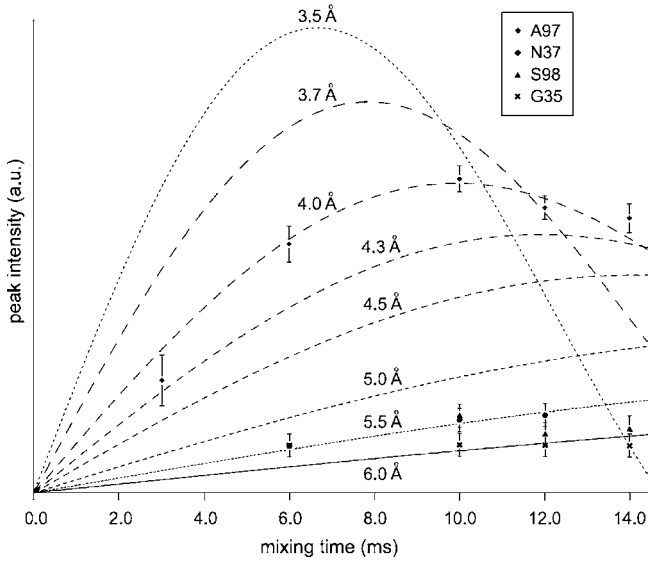

Figure 3. Experimental and simulated TEDOR build-up curves. Experimental peak intensities for G35, N37, A97, and S98 as function of the $^{31}P-^{15}N$ TEDOR mixing time were obtained from a ^{15}N 1D version of the TEDOR experiment.[5] Error bars represent the accuracy of the determined values. The build-up curves were simulated using the software SIMPSON.[28] The best fit of the strongest dipolar coupling between U20-^{31}P and A97-^{15}N yielded a distance of 4.0 (±0.1) Å. From this, the build-up curves of the weakly coupled $^{31}P-^{15}N$ pairs could be translated into relative distances, estimated as 5.5 (±0.5) Å for N37 and S98 and 6.0 (±0.5) Å for G35.

for large RNP complexes, for which the protein nitrogen resonances cannot be assigned in solution, a complete assignment of the protein backbone by ssNMR would be required.

The assignment of the phosphorus resonances is a more challenging task. To date there is no experiment that allows assignment of RNA resonances, and in particular those of the phosphorus nuclei, by ssNMR. In principle, $^{31}P-^{13}C$ correlation experiments, similar to those performed in solution, could be used to assign the phosphorus nuclei in ssNMR. However, the extensive dipolar coupling network of carbon nuclei in the solid-state dictates that selective labeling of specific ribose carbon atoms and/or highly selective transfer schemes are likely to be required. The development of such experiments is ongoing in our laboratory. The current methodology for assigning phosphorus atoms in ssNMR requires systematic substitution of single backbone phosphates by thiophosphates.[27] The substitution of an oxygen atom with sulfur causes a large downfield shift of the phosphorus resonance (∼60 ppm), which makes it readily identifiable. In this work, we did not need to undertake the time-consuming thio-phosphate scanning of the RNA, as the identity of the phosphorus showing contacts with the protein backbone (U20-^{31}P) could be readily recognized by inspection of the crystal structure of the L7Ae−box C/D RNA complex. Instead, we restricted ourselves to assigning the phosphorus spectrum of the L7Ae−box C/D RNA complex in solution and verifying that the solution-state NMR assignment of the U20-^{31}P corresponds to the ^{31}P observed in the solid-state TEDOR spectrum. However, in a real-case scenario, when the structure of the complex is not available, the ssNMR assignment of the ^{31}P nuclei must be verified (or even obtained de novo) by thiophosphate scanning[27] until a more efficient assignment strategy is developed.

In this case, the assignment of the ^{31}P CSs in solution indicates that the U20-^{31}P resonance is high-field-shifted and is the second right-most resonance (Figure S2). In agreement with this, the ^{31}P resonance showing correlations with ^{15}N nuclei in the TEDOR spectrum is shifted to high-field and corresponds to the right-most shoulder of the ^{31}P envelope in the ssNMR ^{31}P 1D spectrum, supporting (but not allowing de novo) its assignment to U20.

Next, we attempted to quantify the distances between the U20-^{31}P and the protein ^{15}N nuclei by comparing the build-up of the TEDOR transfer signals, measured at different mixing times in a ^{15}N 1D version of the 2D experiment, with theoretical transfer curves calculated with SIMPSON[28] (Figure 3). Accurate distances could be extracted for G35, N37, A97, and S98, but not for T36, due to the partial overlap of its resonance with the much more intense resonance of A97. The closest ^{15}N nucleus to U20-^{31}P is that of A97 at 4.0 (±0.1) Å distance, followed by N37 and S98 at ∼5.5 Å and last G35 at ∼6.0 Å distance. This set of measured distances was employed to refine the structure of the *PF* L7Ae−box C/D RNA complex using the crystallographic structure of the homologous *AF* complex as the starting point and using the procedure described in the Methods section. The distance U20-$^{31}P-$T36-^{15}N, which could not be quantitatively measured, was loosely restrained to the range 3.0−6.2 Å. A lower limit of 6.2 Å was also given for the distances U20-$^{31}P-$A96-^{15}N and A19-$^{31}P-$A95-^{15}N, following

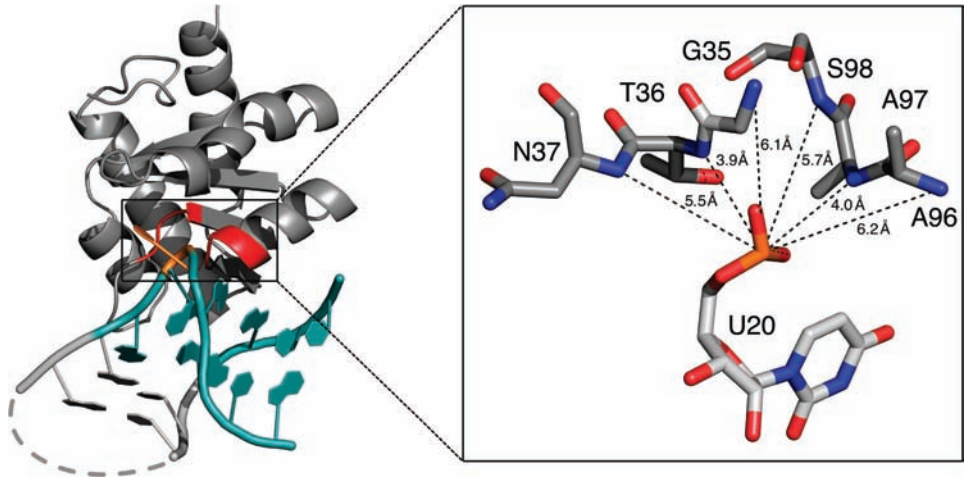

Figure 4. K-turn binding site of *PF* L7Ae. This model was obtained by restrained energy minimization of the X-ray structure of the *AF* binary RNP, as explained in the text. The box C/D region of the RNA is colored in turquoise, the protein region contacting the RNA is in red and the bulged-out U20 is in orange. The distances between the ^{15}N backbone nuclei and the phosphorus of U20 are given in the magnification rectangle.

the absence of the corresponding cross-peaks in the TEDOR spectrum. The resulting model is shown in Figure 4 together with the $^{31}P-^{15}N$ distances measured from the model. As expected, the structure of the *PF* L7Ae−box C/D RNA complex is very close to that of the *AF* complex, with a pairwise backbone rmsd for the protein−RNA interface (including amino acids 34−37, 62 and 94−98 of L7Ae and nucleotides 19 and 20 of the RNA) of only 0.54 Å. However, slight differences are present in the exact geometry of the RNA recognition site, with the N37-^{15}N being substantially closer to the U20-^{31}P in the *PF* (5.5 Å) than in the *AF* (6.0 Å) complex. All distances measured by the ssNMR TEDOR experiment can be well accommodated in the geometry of the protein−RNA recognition site, confirming the reliability of the experimental approach.

Conclusions

Our study demonstrates the potential of ssNMR to study intermolecular interactions in RNP complexes. The $^{31}P-^{15}N$ correlation proposed in this study is highly selective, as proteins do not contain phosphorus, thus ensuring that the observed $^{31}P-^{15}N$ cross-peaks are intermolecular. The efficacy of the methodology is proven here for the binary RNP consisting of the box C/D RNA and the L7Ae protein of *PF*. We show that intermolecular distances between ^{15}N nuclei of L7Ae and the phosphate backbone of the box C/D RNA can be measured and are in very good agreement with those expected from the crystallographic structure of the *AF* L7Ae−box C/D RNA complex. In a general case, ^{31}P (RNA)−^{15}N (protein) distances measured with this approach could be used as restraints in a molecular modeling protocol that builds the RNP complex starting from the structures of the single components.

In this work we have demonstrated the first application of ssNMR spectroscopy to map intermolecular interactions at a protein−RNA binding interface. The principal strength of ssNMR spectroscopy here is that heteronuclei can be directly correlated by dipolar-coupling-mediated correlation spectroscopy so that the density of the structural information is not dependent on the proton distribution. In addition, ssNMR does not require single crystals of particular size and hence is also applicable to RNP complexes that cannot be crystallized. Notably for the binary complex investigated here, single crystals for X-ray crystallography could only be obtained using the *AF* construct,[7] while the precipitation method for solid-state NMR appears to be insensitive to length or sequence deviations of the RNA. Lastly, ssNMR has a much less stringent size limitation than solution-state NMR, being determined solely by the sensitivity of the instrumentation. As a consequence, we foresee that ssNMR methodologies will assume an important role in exploring the three-dimensional architecture of large RNP complexes that tumble too slowly to be suitable for NMR structural investigation in solution and that do not crystallize.

Acknowledgment. This work was supported by the DFG (Grant CA-294/2-1 to T.C.) and by the EMBL. We thank Dr. Wolfgang Bermel at Bruker Biospin for providing measurement time and for continuous discussions.

Supporting Information Available: Figures S1 and S2 and the complete ref 19. This material is available free of charge via the Internet at http://pubs.acs.org.

JA909723F

(27) Olsen, G. L.; Edwards, T. E.; Deka, P.; Varani, G.; Sigurdsson, S. T.; Drobny, G. P. *Nucleic Acids Res.* **2005**, *33*, 3447–3454.
(28) Bak, M.; Rasmussen, J. T.; Nielsen, N. C. *J. Magn. Reson.* **2000**, *147*, 296–330.